

# EUVE Observations of Neutron Stars

Eric J. Korpela and Stuart Bowyer

Space Sciences Laboratory, University of California, Berkeley, CA 94720

## ABSTRACT

We present the results of searches for EUV emission from neutron stars conducted with the EUVE Deep Survey and Scanner Telescopes. To date, 21 fields containing known neutron stars have been observed in the Lexan/Boron (40–190 Å) band. Of these, 11 fields were simultaneously observed in the Aluminum/Carbon (160–385 Å) band. Five neutron stars which have been detected in the EUV have been reported previously; no new detections have been made in the studies reported here. For those sources not detected, we have used the observations to obtain limits on the spectral flux from the neutron stars in these bands. We provide means to convert these fluxes into intrinsic source fluxes for black-body and power law spectra for varying levels of absorption by the interstellar medium.

*Subject headings:* stars: neutron — ultraviolet: stars

## 1. Introduction

The study of EUV emission from neutron stars can address several problems in the astrophysics of neutron stars. Thermal emission from the star can be compared with models of the cooling of neutron star interiors. As processes in the neutron star atmosphere may be important in modifying this thermal radiation, studies of EUV emission can lead to clues to the composition and structure of neutron star atmospheres (Pavlov *et al.*, 1996). For older neutron stars, the possibility of reheating due to internal and external processes can be investigated (Edelstein *et al.*, 1995). In addition magnetospheric processes can contribute to EUV emission, providing constraints on the magnetic field and magnetospheric plasma properties.

Due to interstellar absorption, EUV observations of neutron stars are difficult. The earliest EUV observations of radio pulsars were made by Greenstein *et al.* (1977) using an EUV telescope carried by the Apollo-Soyuz mission. Their observation produced only upper limits to the EUV flux of  $\sim 10^{-12}$  erg/s/cm<sup>2</sup>/Å for three sources. Observations at

soft X-ray bands using Einstein and ROSAT have produced detections of several neutron stars (Ögelman, 1995). The Extreme Ultraviolet Wide Field Camera (WFC) on ROSAT did not report any detection of EUV emission from neutron stars.

A number of neutron stars have been detected in the extreme ultraviolet with the Extreme Ultraviolet Explorer (EUVE) satellite. One of these is in an accretion system (Her X-1) where the bulk of the emission is due to the accretion disc; others are neutron stars radiating thermally or with a nonthermal pulse related emission. All of the detections were made in connection with long duration Guest Observer studies of neutron stars. A number of searches for EUV emission from neutron stars have been carried out. Some of these were short duration exploratory searches of likely candidates carried out by the authors as Guest Observers. Some fields were examined in the EUVE “Right Angle” observation program.

In this paper we provide the results of all the EUVE observations of neutron stars. Twenty fields containing known neutron stars have been observed in the Lexan/Boron (40–190 Å ) band. Of these, 11 were simultaneously observed in the Aluminum/Carbon (160–385 Å ) band. We include the previously reported detections for the purpose of providing a complete sample of the sources observed by EUVE. For those sources not detected, we have used the observations to obtain limits on the spectral flux in the Lexan/Boron and Aluminum/Carbon bands. We present these results and provide means to convert these fluxes into intrinsic source fluxes for black-body and power law spectra, and for varying levels of absorption by the interstellar medium.

## 2. Observations

The EUVE satellite (Bowyer & Malina 1991) offers two observing modes for broadband filter photometry. The primary instrument, the “Deep Survey” telescope, has a high effective area and provides filters for both the 100 Å Lexan/Boron band and the 200 Å Aluminum/Carbon band. These filters cover different portions of the field of view. Therefore a target cannot be simultaneously observed in both bands with the Deep Survey telescope. As the primary science instrument, this telescope is usually used for Guest Observer projects. Some Guest Observer time has been granted to the authors for observations of fields containing neutron stars; we include the results of those observations here.

The EUVE satellite also has 3 “Scanner” telescopes set at right angles to the Deep Survey telescope. The three coaxial telescopes have smaller effective areas, but allow simultaneous observation in both the 100 Å and 200 Å bands. Because the satellite can

rotate around the axis of the Deep Survey telescope, these telescopes may be used when a potentially interesting object falls  $90 \pm 2^\circ$  from a target being observed with the Deep Survey telescope. We (and others) have provided lists of neutron stars for possible observation using this method. Although there is a low probability of any specific target being observed using this approach, a reasonable number of fields have been observed. Because the exposures are usually of the same duration as that of the Deep Survey observation, these observations can be quite long.

The bandpasses in the Deep Survey and Scanner telescopes are defined by thin film filters. The Lexan/Boron 100 Å band extends from 40–190 Å and is sharply peaked at 90 Å. The Aluminum/Carbon 200 Å band extends from 160–385 Å and is peaked at 170 angstroms. The effective areas of these filters are provided in Bowyer *et al.* (1996). Because the variation of the absorption cross section of the interstellar medium with wavelength is substantial in the EUV, differing interstellar absorptions can greatly alter the effective bandpass. This effect will be discussed in Section 3.

The data discussed herein were obtained through the Center for EUV Astrophysics, (CEA) which operates the EUVE satellite. The data were processed through the CEA data pipeline which takes raw satellite data, screens out bad data due to high noise rates or SAA passages, corrects for instrument distortions, and calculates effective exposure times. The output products of this pipeline are images in sky coordinates.

The point spread function (PSF) of the EUVE instruments is  $\sim 30''$  FWHM. This is comparable to the RMS EUVE position error for identified sources of  $\sim 45''$ . Because of these uncertainties, and the fact that the positions of some neutron stars are uncertain by up to several arcminutes, we performed an exhaustive search for point sources within  $\sqrt{1 + \sigma_{\text{psr}}^2}$  arcminutes of the expected neutron star position in the images, where  $\sigma_{\text{psr}}$  is the uncertainty in the neutron star position. In those cases where no sources were found, we present an upper limit which is  $2\sigma$  above the maximum PSF convolved count rate found in the search area. The values for  $\sigma$  are calculated through count statistics using the relation

$$\sigma = \sqrt{N_{fg} + N_{bg} \frac{A_{psf}^2}{A_{bg}^2}} \quad (1)$$

where  $N_{fg}$  indicates the number of counts in a PSF convolved bin of given coordinates and  $N_{bg}$  is the number of counts in a background annulus of inner radius  $1'$  and outer radius  $3'$  centered on the same coordinates.  $A_{psf}$  is the effective solid angle of the autoconvolved PSF ( $\sim 1.2 \text{ arcmin}^2$ ), and  $A_{bg}$  is the solid angle of the background annulus ( $\sim 25 \text{ arcmin}^2$ ). In cases where an object was located near the edge of the detector or in a region of rapidly varying background, the size and shape of the background region was modified, either by

moving the background annulus to an unaffected region, or changing the inner and outer radii of the annulus. The error calculations were modified accordingly to consider the solid angle of the new background region. The count rate measurements or upper limits were corrected for instrument vignetting and instrument dead-time and converted to a mean spectral flux over the measurement bandpass by dividing by the integrated effective area (Edelstein *et al.* (1995), EUVE GO Handbook (1997)) and multiplying by the bandpass mean photon energy. The results are shown in Table 1, accompanied by relevant data on the neutron star obtained from a variety of sources. For those sources which had been previously detected, we provide the previously measured count rate and a calculation of flux using the method described above.

### 3. Discussion

The limits obtained here may or may not be important in constraining models of pulsar structure and emission mechanisms. The importance depends upon the emission model, the distance to the pulsar, and the interstellar absorption in the direction of the pulsar. Because these values are, in general, unknown, we provide factors to convert the measured EUV flux into an intrinsic source flux over a range of values.

Because the opacity is large in the EUV and varies rapidly with wavelength ( $\kappa \approx \lambda^3$ ), an approximation of constant opacity over the bandpass is not applicable. Increasing absorption by the interstellar medium has the effect of reducing the effective area of the EUV telescopes at longer wavelengths. This shifts the peak and mean wavelengths of the effective bandpass to shorter wavelengths. Because of this effect, the intrinsic spectral shape of the source has an impact upon how greatly the source is affected by the absorption. For example, a  $10^5$  K black-body is more affected than a  $10^6$  K black-body because it emits more energy at longer wavelengths. Unfortunately, there is no good analytical approximation for these effects. Using the interstellar opacity cross sections of Rumph *et al.* (1994), we have calculated the effects of interstellar absorption on the measured count rate for a variety of hydrogen column densities for both black-body and power law spectra. We have incorporated these results in conversion factors (discussed below) which allow one to convert the measured flux to an intrinsic flux for a range of black-body temperatures and power law indices.

In Figure 1 we show the conversion factor  $C_{100}^{bb}$  required to convert the measured 100 Å flux to an intrinsic unabsorbed flux at 100 Å for a black-body at a given temperature, using the relationship  $F_o(100 \text{ Å}) = C_{100}^{bb} F_{100}$ . We obtained this conversion factor by calculating an absorbed black-body spectrum and determining the associated Lexan band count rate.

Table 1: EUVE observations of neutron star fields

Name	Duration (s)	Lex ( $10^{-3}c/s$ )	$F_{100}$ ( $erg/s/cm^2/\text{\AA}$ )	Al/C ( $10^{-3}c/s$ )	$F_{200}$ ( $erg/s/cm^2/\text{\AA}$ )	DM ( $cm^{-3}pc$ )	$\mu$ (mas/yr)	$\pi$ (mas)	Notes	Other Names	Refs.
J0006+1834	47771	< 0.57	< $1.4 \times 10^{-16}$	< 0.68	< $3.8 \times 10^{-16}$	$12.0 \pm 0.6$			S		5
J0108-1431	119064	< 0.38	< $1.8 \times 10^{-17}$			$1.83 \pm 0.02$			DS		6
J0152-1637	19208	< 0.99	< $4.6 \times 10^{-17}$			$11.94 \pm 0.04$	$150 \pm 50$		DS		7
J0304+1932	39060	< 0.67	< $1.7 \times 10^{-16}$	< 0.58	< $3.3 \times 10^{-16}$	$15.69 \pm 0.05$	37		S		7
J0437-4715	71886	$14.3 \pm 0.8$	$6.6 \pm 0.4 \times 10^{-16}$			2.64	135	$5.6 \pm 0.8$	DS		8
J0459-0210	171803	< 0.80	< $2.0 \times 10^{-16}$	< 1.23	< $6.8 \times 10^{-16}$	$14 \pm 3$			S		9
J0633+1746	250458	$8.1 \pm 0.2$	$3.8 \pm 0.1 \times 10^{-16}$				108	$6.3 \pm 1.7$	DS	Geminga	1,3
J0659+1414	91021	$23.2 \pm 0.6$	$1.08 \pm 0.03 \times 10^{-15}$			$14.02 \pm 0.05$	70		DS	B0656+14	1,10
J0837+0610	43724	< 0.53	< $1.3 \times 10^{-16}$	< 0.57	< $3.2 \times 10^{-16}$	12.85	51		S		11
J1025-0709	100801	< 0.93	< $4.3 \times 10^{-17}$			$6.4 \pm 0.5$			DS		12
J1239+2453	69805	< 0.47	< $1.2 \times 10^{-16}$	< 0.49	< $2.7 \times 10^{-16}$	9.28	114		S		7,11
J1455-3330	322558	< 0.37	< $9.2 \times 10^{-17}$	< 0.28	< $1.6 \times 10^{-16}$	13.57			S		13
J1607-0032	155855	< 0.45	< $1.1 \times 10^{-16}$	< 0.44	< $2.4 \times 10^{-16}$	10.68	$7 \pm 17$		S		11
J1657+3520	(a)	$180 \pm 12$	$4.4 \pm 0.3 \times 10^{-14}$						DS	Her X-1	4
J1713+0747	43880	< 0.68	< $1.7 \times 10^{-16}$	< 0.56	< $3.1 \times 10^{-16}$	15.99	6		S		14
J1856-3754	582000	$38.4 \pm 0.3$	$1.78 \pm 0.01 \times 10^{-15}$						DS	RX J185635-3754	2
J1908+0734	257210	< 0.31	< $7.7 \times 10^{-16}$	< 0.37	< $2.1 \times 10^{-16}$	$11.10 \pm 0.01$			S		5
J1932+1059	43482	< 0.92	< $4.2 \times 10^{-17}$			3.18	106	18.2(b)	DS		12
J2124-3358	17164	< 1.49	< $6.9 \times 10^{-17}$			4.41			DS		12
J2144-3939	19921	< 1.50	< $7.0 \times 10^{-17}$			$4 \pm 4$			DS		9,12
J2155-5641	103132	< 0.37	< $9.2 \times 10^{-17}$	< 0.39	< $2.2 \times 10^{-16}$	$14 \pm 9$			S		15

References for Table 1.

(all) Taylor *et al.* (1993,1997); (1) Foster *et al.* (1996); (2) Walter *et al.* (1996); (3) Bignami *et al.* (1996); (4) Vrtilik *et al.* (1994); (5) Camilo & Nice (1995); (6) Tauris *et al.* (1994); (7) Fomalont *et al.* (1992); (8) Bell *et al.* (1995); (9) Manchester *et al.* (1996); (10) Thompson & Córdova (1994); (11) Phillips & Wolszczan (1992); (12) Lorimer *et al.* (1995); (13) Lorimer *et al.* (1995b); (14) Camilo *et al.* (1994); (15) Newton *et al.* (1981).

Notes to Table 1.

(a) No value given; (b) No uncertainty given; (S) Scanner Observation; (DS) Deep Survey Observation

This count rate was converted to a band averaged flux by dividing by the integrated effective area of the Lexan band. The ratio of the unabsorbed flux to this averaged flux is the conversion factor. The conversion factor is plotted for neutral hydrogen column densities of  $0, 10^{19}, 10^{19.5}, 10^{20}$ , and  $10^{20.5}$ . Note that these conversion factors can be less than unity in those cases where the emission is predominantly at wavelengths longer than the bandpass central wavelength. In Figure 2 we show the equivalent conversion factors for the 200 Å band.

In Figure 3 we show the 100 Å band conversion factors  $C_{100}^{pl}$  for power law spectra of the form  $F_{\lambda} = F_o \left(\frac{\lambda}{\lambda_o}\right)^{\alpha}$  for power law indices between -4 and 4. In Figure 4 we show the equivalent conversion factors for the 200 Å band.

#### 4. Summary

We present the results of searches for EUV emission from 21 neutron stars. Five neutron stars (reported previously) have been detected with EUVE in the 100 Å Lexan/Boron band. We provide measured fluxes for these sources and upper limit fluxes for the remaining objects which have not been detected. We also provide upper limit fluxes in the 200 Å Aluminum/Carbon band for those sources which were observed in that band. Of the five detected neutron stars, one is an active accretion source (Her X-1), one is a millisecond pulsar (J0437-4715), two are isolated pulsars (Geminga, J0659+1414), and one is an thought to be an isolated, non-pulsing neutron star (RX J185635-3854).

We thank Michael Lampton for useful comments. This work has been supported by NASA grant NAS5-30180.

#### REFERENCES

- Bell, J. F., Bailes, M., Manchester, R. N., Weisberg, J. M., & Lyne, A. G. 1995, ApJ, 440, L81
- Bignami, G. F., Mignani, R., Edelstein, J., & Bowyer S. 1996, ApJ, 456, L111
- Bowyer, S., & Malina, R. F. 1991, in Extreme Ultraviolet Astronomy, ed. Malina & Bowyer, (New York: Pergamon), 397
- Bowyer, S., Lampton, M., Lewis, J., Wu, X., Jelinsky, P., & Malina, R. F. 1996, ApJS, 102, 129

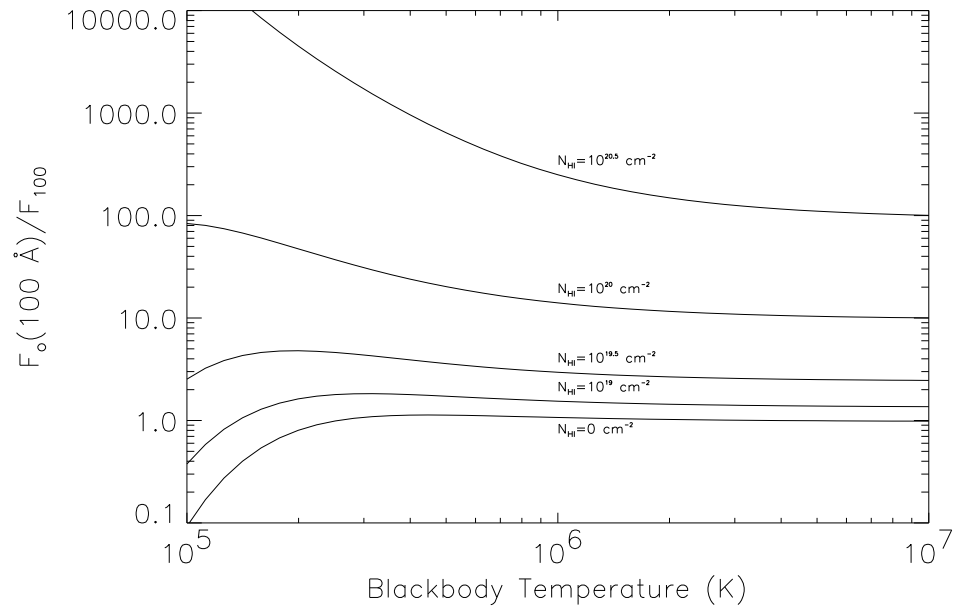


Fig. 1.— Lexan/Boron band absorption conversion factors for black-body spectra.

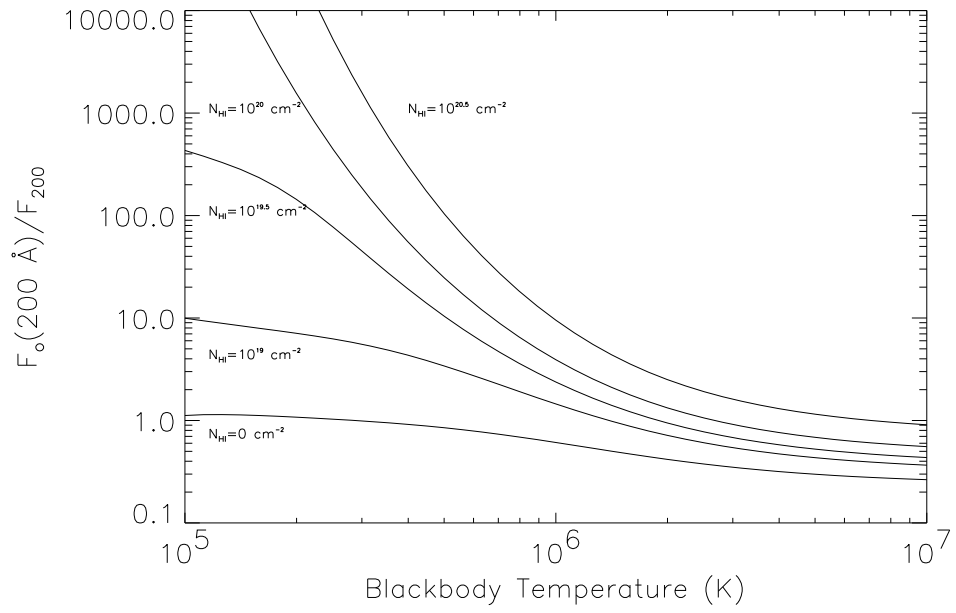


Fig. 2.— Aluminum/Carbon band absorption conversion factors for black-body spectra.



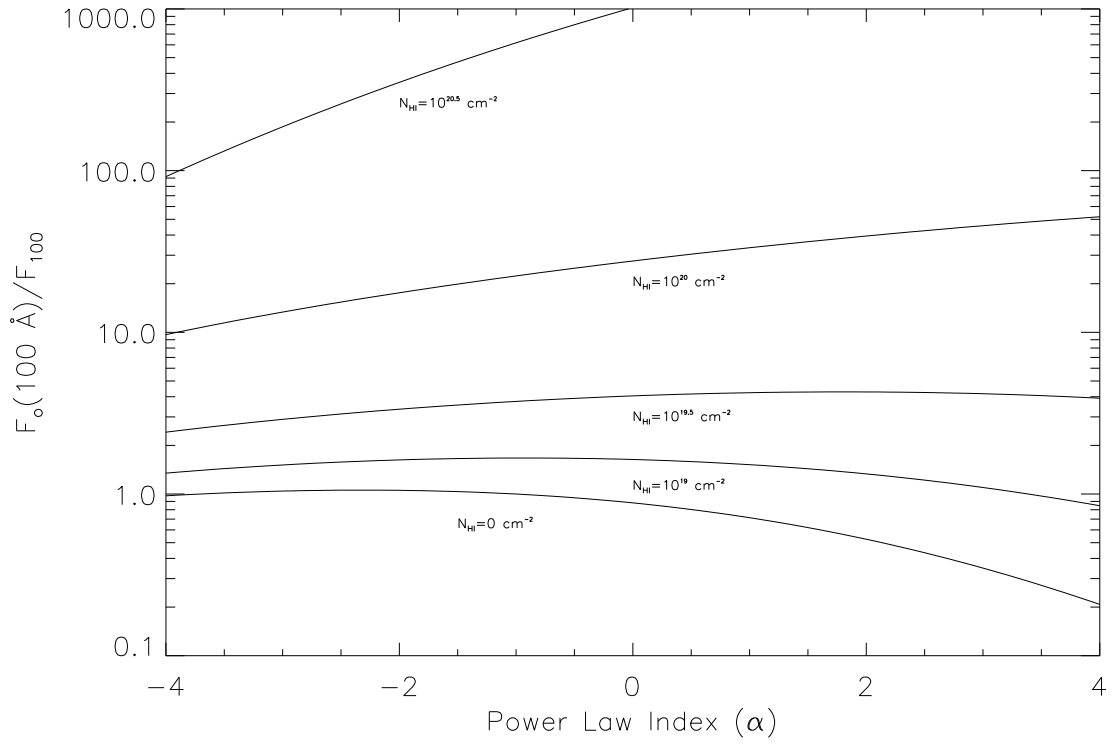


Fig. 3.— Lexan/Boron band absorption conversion factors for power law spectra.

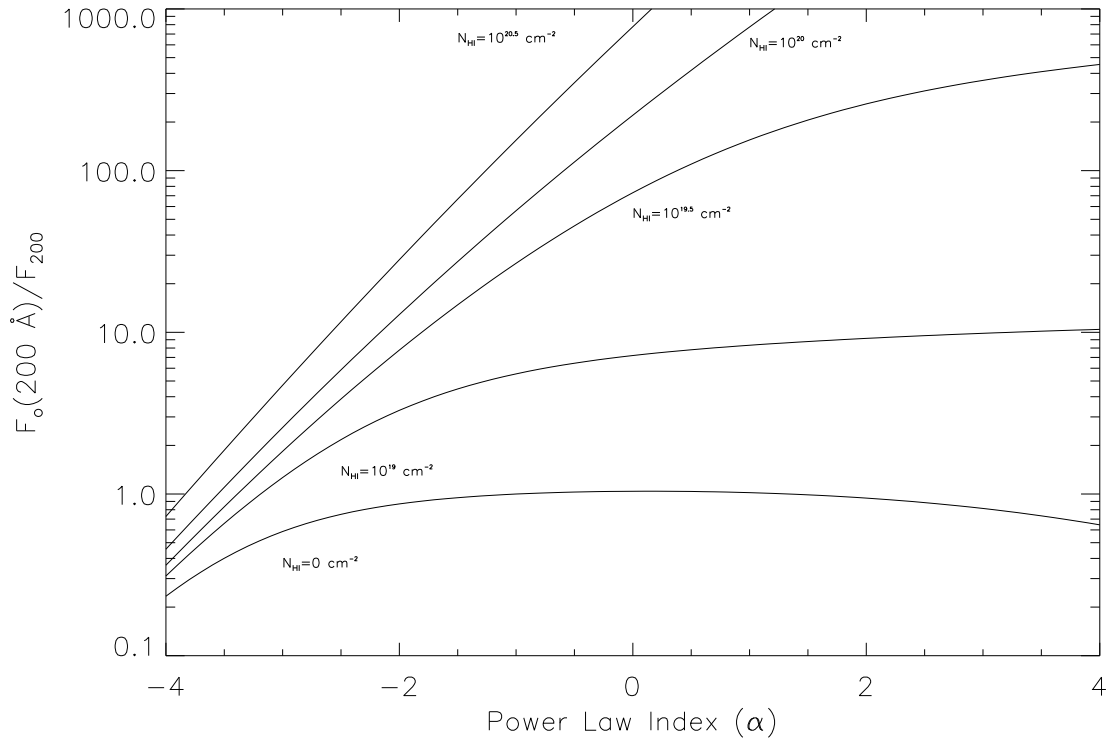


Fig. 4.— Aluminum/Carbon band absorption conversion factors for power law spectra.

- Camilo, F., Foster, R. S., & Wolszczan, A. 1994, ApJ, 437, L39
- Camilo, F., and Nice, D. J. 1995, ApJ, 445 756
- Edelstein, J., Foster, R. S., & Bowyer, S. 1995. ApJ 454, 442
- EUVE Guest Observer Center. 1997, EUVE Guest Observer Program Handbook, 97-EUVE-06, [http://www.cea.berkeley.edu/~science/html/Resources\\_pubs\\_handbook.html](http://www.cea.berkeley.edu/~science/html/Resources_pubs_handbook.html)
- Fomalont, E. B., Goss, W. M., Lyne, A. G., Manchester, R. N., & Justtanont, K. 1992 MNRAS, 258, 497
- Foster, R. S., Edelstein, J., & Bowyer, S. 1996, Proc. IAU Colloq. 152, Astrophysics in the Extreme Ultraviolet, ed. S. Bowyer & R. F. Malina (Dordrecht: Kluwer Academic Publishers), 437
- Greenstein, G., Margon, B., Bowyer, S., Lampton, M., Stern, R., & Gordon, K. 1977, A&A, 54, 623
- Lorimer, D. R., Yates, J. A., Lyne, A. G., & Gould, D. M. 1995, MNRAS, 273, 411
- Lorimer, D. R., Nicastro, L., Lyne, A. G., Bailes, M., Manchester, R. N., Johnston, S., Bell, J. F., D’Amico, N., & Harrison, P. A. 1995, ApJ, 439, 933
- Manchester, R. N., Lyne, A. G., D’Amico, N., Bailes, M., Johnston, S., Lorimer, D. R., Harrison, P. A., Nicastro, L., & Bell, J. F. 1996, MNRAS, 279, 1235
- Newton, L. M., Manchester, R. N., & Cooke, D. J. 1981, MNRAS, 194, 841
- Ögelman, H. 1995, in Lives of Neutron Stars, ed. N. A. Alpar, U. Kiziloglu, & J. van Paradijs, NATO ASI Ser, C, 450, 101
- Pavlov, G. G., Zavlin, V. E., Trümper, J. & Neuhäuser, R. 1996, ApJ, 472, L33
- Phillips, J. A., & Wolszczan, A. 1992, ApJ 385, 273
- Rumph, T., Bowyer, S., & Vennes, S. 1994, AJ, 107, 2108
- Tauris, T. M., Nicastro, L., Johnston, S., Manchester, R. N., Bailes, M., Lyne, A. G., Glowacki, J., Lorimer, D. R., & D’Amico, N. 1994, ApJ, 428, L53
- Taylor, J. H., Manchester, R. N., & Lyne, A. G. 1993, ApJS, 88, 529
- Taylor *et al.* 1997, The Princeton Pulsar Catalog, <http://pulsar.princeton.edu/pulsar/catalog.shtml>

Thompson, R. J., and Córdoba, F. A. 1994, *ApJ*, 421, L13

Walter, F. M., Wolk, S. J., & Neuhäuser, R. 1996, *Nature*, 379, 233

Vrtilek, S. D., Mihara, T., Primini, F. A., Kahabka, P., Marshall, H., Agerer, F., Charles, P. A., Cheng, F. H., Dennerl, K., la Dous, C., Hu, E. M., Rutten, R., Serlemitsos, P., Soong, Y., Stull, J., Trümper, J., Voges, W., Wagner, R. M., & Wilson, R. 1994, *ApJ*, 436, L9